Etch features in Czochralski-grown single crystal indium phosphide

G. T. BROWN, B. COCKAYNE, W. R. MacEWAN
Royal Signals and Radar Establishment, St Andrews Road, Malvern, Worcs

Two etchants for InP have been used to categorize etch features in both horizontal and vertical sections of InP single crystals grown by the Czochralski liquid encapsulation technique; these are the AB etchant, used extensively for defect analysis in GaAs and another etchant based on a phosphoric acid/hydrobromic acid mixture. The behaviour of these etchants is different but a cross correlation has been made between the types of etch feature produced. Transmission X-ray topography has been used to correlate etch features with dislocations. Nominally undoped crystals and material doped with specific impurities, e.g. Fe, Ge, Zn, have been examined. The principal features produced by etching are pits, ridges and striations. It is shown that the density and distribution of pits and ridges is consistent with these features being dislocation structures and the mechanisms by which they are revealed are discussed in terms of etching rates. The results allow comment to be made upon interface shape and the source of dislocations in InP crystals grown by the Czochralski technique.

1. Introduction

Single crystal indium phosphide (InP) grown by the Czochralski liquid encapsulation method is now used extensively as a substrate material for composite layer devices such as transferred electron oscillators, field effect transistors and heterostructural lasers. In all these devices the presence of defects in the substrate which may propagate into epitaxial layers grown thereon is potentially detrimental to device performance. A prerequisite for controlling defects is to have some convenient means by which the nature and distribution of defects can be assessed. One such way is to use a chemical etchant which will reveal and also differentiate between the types of defect present; this technique has been used extensively for other III–V compounds but particularly for gallium arsenide [1]. Several etchants for InP have been proposed [2–5] but so far there has been no substantial correlation between the features produced by these etchants and no systematic study of single crystals has been reported. In the present study, the two more extensively used etchants [4, 6] have been used to characterize both nominally undoped single crystals and material doped with germanium and iron.

2. Experimental technique

Single crystals of InP were prepared using the liquid encapsulation Czochralski (LEC) technique [2] incorporating the crucible weighing method of automatic diameter control [7]. The doping levels and electrical characteristics of the crystals examined are listed in Table 1. In this work only crystals which were completely twin free were examined. Orientated 1 mm thick slices were cut from the top and bottom of crystals grown along both ⟨100⟩ and ⟨111⟩ directions. Transverse sections were usually cut perpendicular to the crystal axis but for comparison some {111} slices were cut from ⟨100⟩ crystals and vice-versa. Longitudinal sections were cut parallel to {110} planes. The slices were ground initially on fine silicon carbide to remove any surface irregularities introduced by sawing and then chemically polished in a weak solution of bromine in methanol on a pellon pad to remove a further 250 μm of material in order to avoid residual work damage. Each slice was thorougly cleansed in boiling trichorethylene, acetone and propan-2-ol prior to etching. Specimens for X-ray topography were prepared by polishing to a thickness of 200 μm with a bromine–methanol solution on a pellon pad.

TABLE I Data pertaining to material examined in the present study

Crystal number	Dopant	Orientation	Carrier concentration (cm^{-3})		Mobility ($cm^2V^{-1}sec^{-1}$)		Resistivity (ohm-cm), 77 K
			300 K	77 K	300 K		
149	Sn	⟨111⟩	–	–	–	–	–
251	undoped	⟨100⟩	1×10^{16}	1×10^{16}	–	–	–
758	Ge	⟨111⟩	1.4×10^{17}	2.2×10^{17}	3090	2995	0.01
884	Fe	⟨100⟩	–	–	–	–	2.7×10^{6}
885	undoped	⟨100⟩	5.0×10^{15}	4.0×10^{15}	4912	27253	0.26
887	Ge	⟨100⟩	5.3×10^{16}	3.8×10^{16}	4036	7072	0.02

The etchants used were solution H [4], a mixture of hydrobromic acid and electronic grade orthophosphoric acid in the volumetric proportions of 1:2 respectively, and solution A–B [7], a mixture containing 1 g chromium trioxide, 8 mg silver nitrate dissolved in 2 ml of deionised water and 1 ml of 47% hydrofluoric acid. Typical etching conditions for solution H were 1 to 2 min at room temperature and for solution A–B were 30 to 90 min at 60° C with changes of solution at regular intervals of 10 min in the latter case. The etchants were used individually and in consecutive combinations.

3. Results

3.1. Features revealed by solution H

The general distribution of features produced by solution H on a {100} transverse section of a ⟨100⟩ axis crystal is shown in Fig. 1. The four-fold symmetry in the pattern of etch features is consistent with the formation of dislocations by slip on the {111} ⟨110⟩ systems [8] which is well established behaviour for materials such as InP which have the sphalerite structure. The density of pits plotted across typical ⟨110⟩ and ⟨100⟩ crystal diameters in Fig. 2 shows a distribution which is the same as that predicted for dislocations generated by thermal stresses where radial heat losses predominate [9]. Fig. 2 shows that the mean density of pits is the same for slices of comparable diameter, varying only within very narrow limits and being relatively unchanged by the small amount of dopant required to produce n-conducting (Ge-doped at 10^{16} atom cm^{-3}) and semi-insulating (Fe-doped at 10^{16} atoms cm^{-3}) InP.

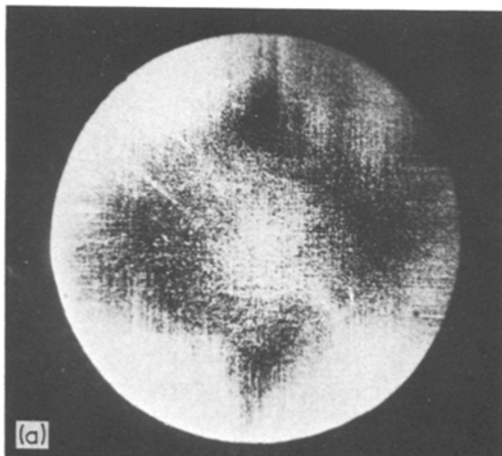

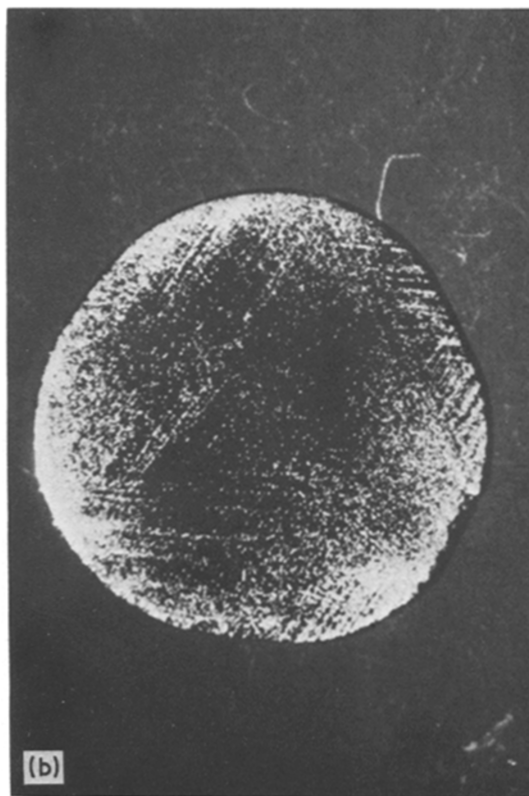

Figure 1 Dark field optical micrographs of (a) a {100} slice cut from an undoped ⟨100⟩ axis crystal etched for 1.5 min in solution H, (b) a {111}P slice cut from a Ge-doped ⟨111⟩ axis crystal etched for 60 min in solution A–B at 60° C.

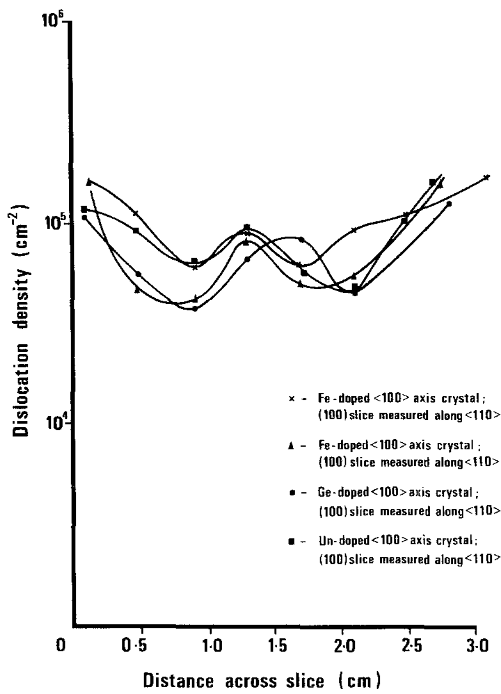

Figure 2 Dislocation density profiles for different crystals.

Closer inspection of Fig. 3a shows that the most predominant feature produced by this etchant is an approximately conical shaped pit (A in Fig. 3a) which tends towards a triangular section on {1 1 1}P surfaces and a square section on {1 0 0} surfaces; the density of these features is typically between 10^4 and $10^5\,cm^{-2}$. This etchant also produces shallow pits (B in Fig. 3a) with an almost circular section within which conical pits can sometimes be found (C in Fig. 3a); the density of shallow pits is typically $10^4\,cm^{-2}$. In the original work using this etchant [4] both of these types of pits were identified but shallow pits were only observed on thin layers whereas in the present study shallow pits were found on undoped material as well as iron and germanium doped substrate surfaces.

If the electronic grade orthophosphoric acid is replaced by a less pure grade a further etch feature may be produced by the etchant. It occurs as a faceted hillock with morphologies which differ slightly on {1 1 1}P and {1 0 0} surfaces. On {1 1 1}P the hillock has a base approximating to a regular hexagon (Fig. 4a) whereas on {1 0 0} the base of the hillock is hexagonal but elongated along one of the ⟨1 1 0⟩ directions (Fig. 4b). The hillocks sometimes appear as clusters in which hillocks merge along their faceted sides (Fig. 4b). On {1 1 1}P surfaces these hillocks are frequently associated with conical pits but no such correlation has been observed for {1 0 0} surfaces. They occur on undoped as well as Fe-, Ge- and Sn-doped crystals and have an irregular distribu-

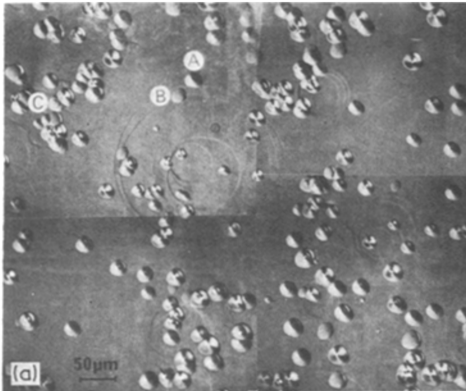

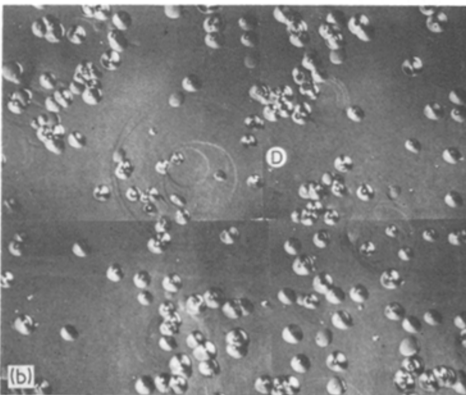

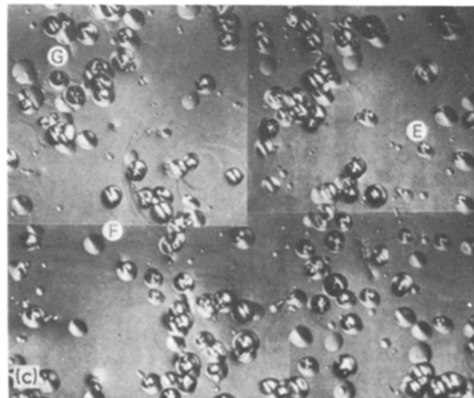

Figure 3 Etch features produced on a {1 1 1}P surface of a Ge-doped ⟨1 1 1⟩ axis crystal by etching for a) 45 sec in solution H, b) 45 sec in solution H and a further 25 min in solution A–B at 60° C, c) 45 sec in solution H and a further 85 min in solution A–B at 60° C.

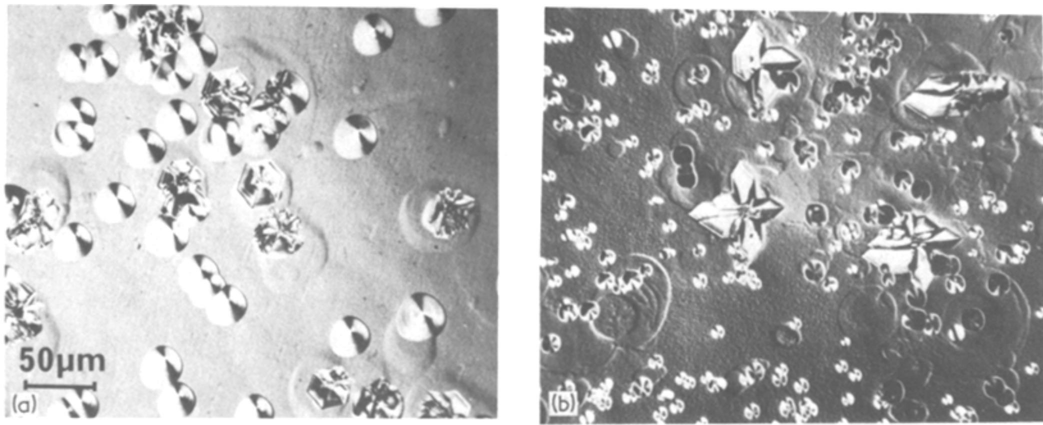

Figure 4 Faceted hillocks produced by etching for 1.5 min in solution H for (a) the {1 1 1}P surface of a Ge-doped ⟨1 1 1⟩ axis crystal, (b) the {1 0 0} surface of a Sn-doped ⟨1 0 0⟩ axis crystal.

tion with a density of 3 to $6 \times 10^3 cm^{-2}$. Upon repeated etching it proved possible to etch through hillocks, some obviously disappearing whilst new ones formed in different areas. Several slices containing hillocks were examined by scanning electron microscopy using EDAX (energy dispersive analysis of X-rays) with a windowless detector. This generally showed that the hillocks were constituted of indium and phosphorus in a ratio comparable to that of the matrix. However, in some instances a very small carbon peak was found to be associated with these features. It is not known whether this observation is meaningful as carbon is a persistent surface contaminant. Thus far it has not proved possible to show conclusively whether these faceted hillocks represent a defect or an etching artefact. It is, however, clear that the use of lower grade orthophosphoric acid significantly modifies the chemical composition of the etch which is manifested in a deeper yellow colouration and leads to the production of these faceted hillocks.

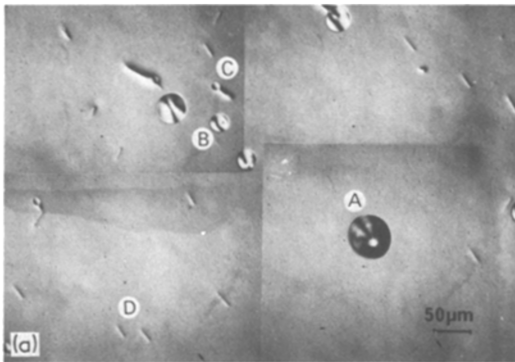

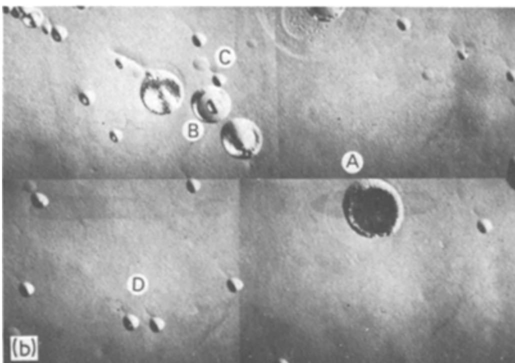

3.2. Features revealed by solution A–B

The general distribution of features produced by solution A–B on a {1 1 1}P transverse section of a

Figure 5 Etch features produced on a {1 1 1}P surface of a Ge-doped ⟨1 1 1⟩ axis crystal by etching for (a) 60 min in solution A–B at 60° C, (b) 60 min in solution A–B at 60° C followed by a further 30 sec in solution H, (c) 60 min in solution A–B at 60° C.

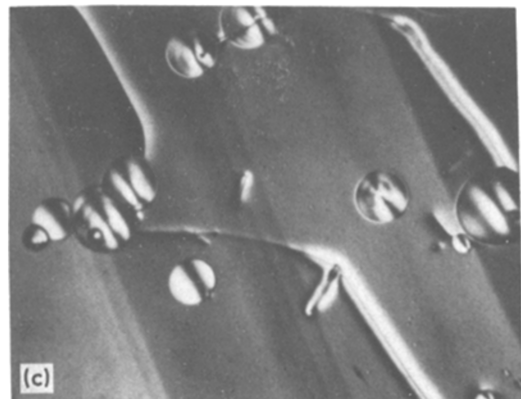

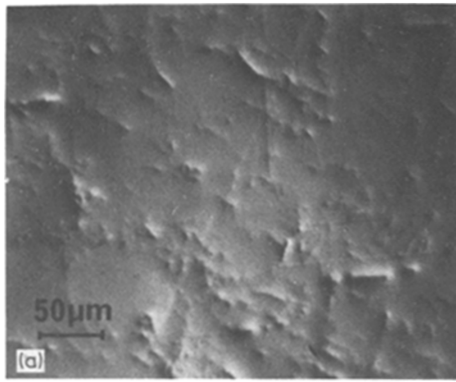

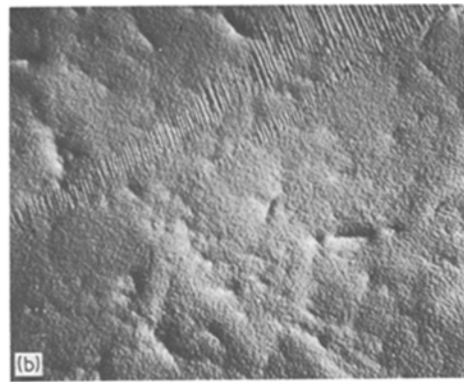

Figure 6 Etch features produced on {1 0 0} surface of a Ge-doped ⟨1 0 0⟩ axis crystal etched for (a) 60 min in solution A–B at 60° C, (b) 60 min in solution A–B at 60° C and a further 40 sec in solution H, (c) 60 min in solution A–B at 60° C and a further 100 sec in solution H.

⟨1 1 1⟩ axis crystal is shown in Fig. 1b. The 3-fold pattern of pits is consistent with dislocation generation by slip in much the same manner as that described in Section 3.1. for solution H. Prolonged etching (60 min) of the {1 1 1}P surface produced several features as listed below.

(i) Conical pits, some with acentric vertices which have a typical density of $2 \times 10^4 \text{cm}^{-2}$ at the crystal edge and $2 \times 10^3 \text{cm}^{-2}$ at the crystal centre. The pits, illustrated (A) in Fig. 5, are identical in appearance to those produced by solution A–B on {1 1 1}As surfaces of GaAs [7] which have been attributed to dislocations emerging normal to the surface.

(ii) Shallow circular pits (B) in Fig. 5a, resembling the shallow pits produced by solution H, which have a density of about 10^3cm^{-2} and a regular distribution apart from a slight increase in density towards the edges of the slice. Some of these pits have an associated ridged "tail" (C) in Fig. 5a, the ridge character of the tail being apparent from the opposite contrast to that given by the pit; the density of these features is approximately $2 \times 10^2 \text{cm}^{-2}$.

(iii) Straight ridges unassociated with pits which have a length of about 20 μm (D) in Fig. 5a, and show alignment with ⟨1 1 2⟩ directions which precludes {1 1 1} planes as the plane containing the defect responsible for these straight ridges. Some longer ridged features showing little alignment are also present. This type of feature (Fig. 5c) shows marked similarity to those produced on {1 1 1}As and {1 0 0} surfaces of GaAs and referred to as an etch-memory feature [10] because it delineates the trace of a dislocation through the material removed by the etchant.

(iv) Growth striations, which can be seen clearly in the background of Fig. 5c; These are discussed separately in Section 4.

In order to examine the role of crystal growth orientation upon etch feature formation a {1 1 1}P slice was cut from a ⟨1 0 0⟩ axis crystal and the {1 1 1}P surface was polished and etched as for the {1 1 1}P slice from a ⟨1 1 1⟩ axis crystal. In fact, all of the features listed from (i) to (iv) were again revealed with the exception of the short straight ridges. The growth striations were also more pronounced.

In contrast to solution H, the etching behaviour of solution A–B on {1 0 0} surfaces is markedly different from that on {1 1 1}P, the most prominent feature being ridges produced by the etch-memory effect (Fig. 6a). No conical or shallow pits form on {1 0 0} surfaces. This behaviour again corresponds to that of GaAs {1 0 0} surfaces. An additional feature on {1 0 0} surfaces occurred in undoped crystals grown directly from polycrystalline material which is slightly rich in In. This is the decorated type of ridge shown in Fig. 7. Undoped crystals produced using Czochralski

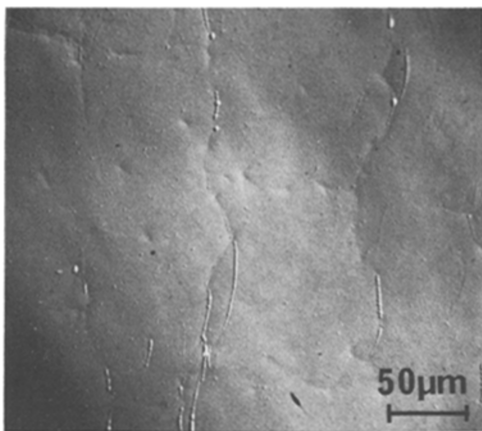

Figure 7 Decorated ridge features produced on a {1 0 0} surface of a ⟨1 0 0⟩ axis undoped "once pulled" crystal after etching for 60 min in solution A–B at 60° C.

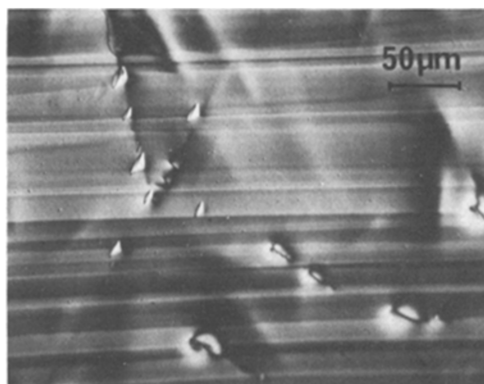

Figure 8 Etch features produced on the {1 1 0} surface of a Ge-doped ⟨1 1 1⟩ axis crystal etched for 90 min in solution A–B at 60° C.

crystals as the starting material did not exhibit this decoration, hence the feature could be associated with excess indium. The etching behaviour of {1 0 0} slices cut from ⟨1 1 1⟩ axis crystals was identical to that described above for {1 0 0} slices cut from ⟨1 0 0⟩ axis crystals except for the enhancement of growth striae.

Etched {1 1 0} slices revealed ridge features but some have hillocks and boat shaped pits associatied with them as illustrated in Fig. 8.

3.3. Combination etching

The work described so far demonstrates that the etching behaviour of both {1 1 1}P surfaces and {1 0 0} surfaces cut from an Fe-doped ⟨1 0 0⟩ crystal H. A combination etching procedure has therefore been used to determine the correlation between the features observed in the two solutions.

In Fig. 3a the {1 1 1}P surface of a Ge-doped ⟨1 1 1⟩ axis crystals has been etched for 1 min in solution H and the familiar conical and flat

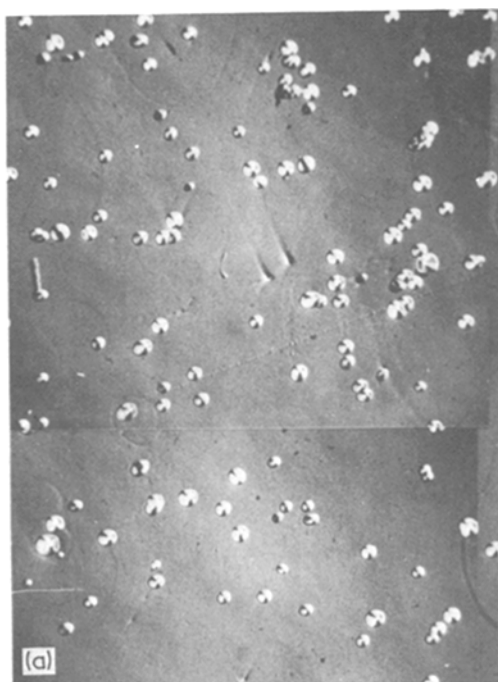

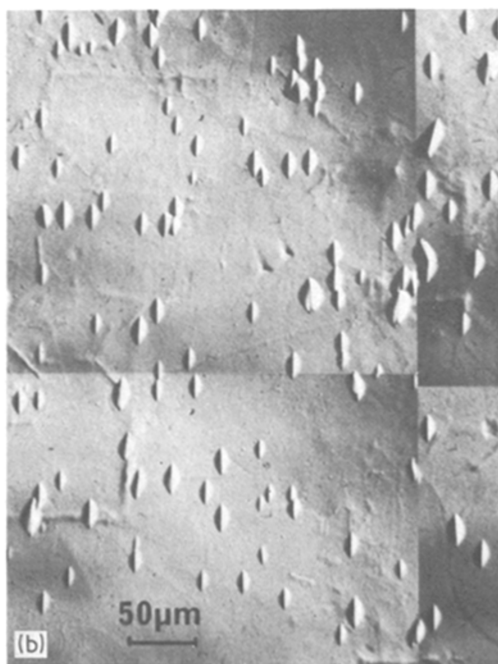

Figure 9 Etch features produced on a {1 0 0} surface taken from an Fe-doped ⟨1 0 0⟩ axis crystal etched for (a) 1 min in solution H, (b) 1 min in solution H followed by 30 min in solution A–B at 60° C.

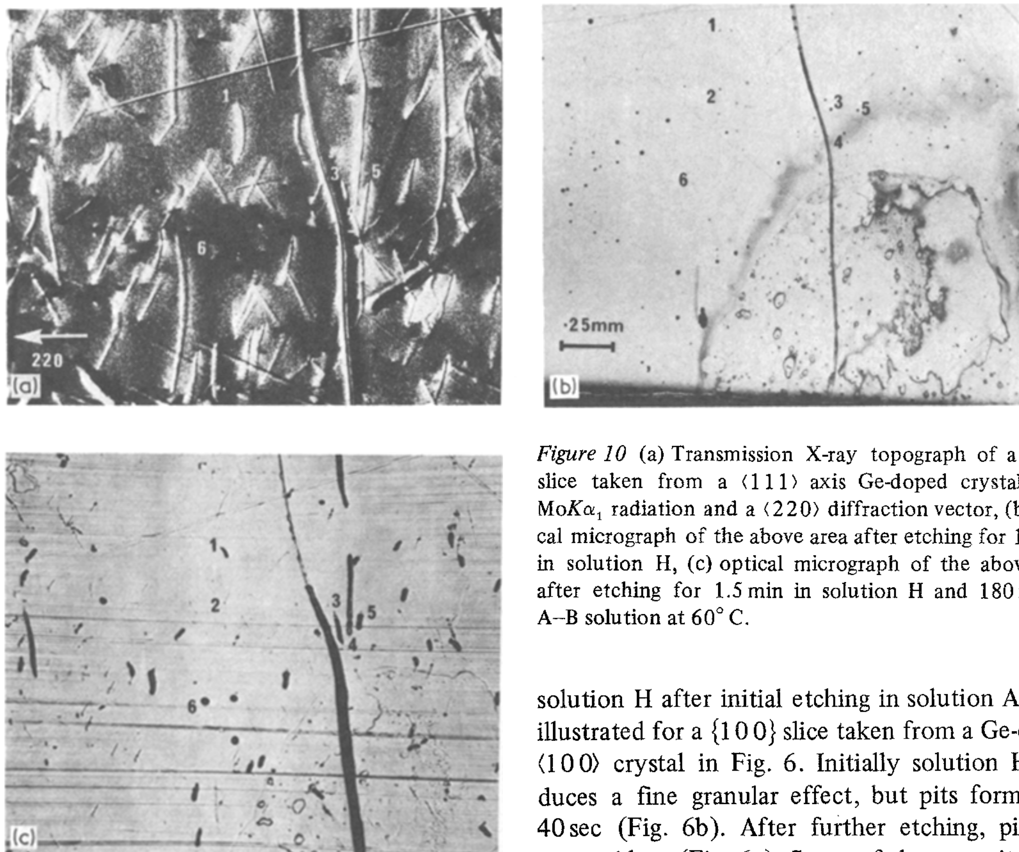

Figure 10 (a) Transmission X-ray topograph of a ⟨100⟩ slice taken from a ⟨111⟩ axis Ge-doped crystal using $MoK\alpha_1$ radiation and a ⟨220⟩ diffraction vector, (b) optical micrograph of the above area after etching for 1.5 min in solution H, (c) optical micrograph of the above area after etching for 1.5 min in solution H and 180 min in A–B solution at 60° C.

bottomed pits are observed (A and B in Fig. 3a). After etching in solution A–B, as illustrated in Fig. 3b, both of these types of pit grow larger which suggests a correlation between these features in the two etchants. However it is also evident that a number of new shallow pits occur after etching in solution A–B (Fig. 3b, D). New conical pits also appear within existing conical and shallow pits produced by solution H (E in Fig. 3c); however this is not true for all pits (e.g. F in Fig. 3c). After prolonged etching (85 min), the characteristic ridges (G in Fig. 3c) appear and, although not clearly evident in Fig. 3, growth striations were also detectable.

The effect of the same combination etching on {100} surfaces cut from an Fe-doped ⟨100⟩ crystal is shown in Fig. 9. Fig. 9b depicts the effect of etching in A–B solution. The general effect is for conical and flat bottomed pits to adopt a boat-shape with elongation in the ⟨1 1 0⟩ direction whilst etch-memory ridge features start to develop after prolonged etching. Some of the ridges are associated with etch pits as can be seen in Fig. 9b.

The reverse procedure, with succesive etching in solution H after initial etching in solution A–B, is illustrated for a {1 0 0} slice taken from a Ge-doped ⟨1 0 0⟩ crystal in Fig. 6. Initially solution H produces a fine granular effect, but pits form after 40 sec (Fig. 6b). After further etching, pits are very evident (Fig. 6c). Some of the new pits form at the end of the etch-memory ridge features which tend to disappear gradually after continued etching.

The same etching procedure for a {1 1 1}P surface from a Ge-doped ⟨1 1 1⟩ crystal is illustrated in Figs. 5a and b. The large conical pits formed by etching in solution A–B grow larger (A in Fig. 5) and develop a granular surface on etching in solution H. The flat bottomed pits (B in Fig. 5) retain their shape but some form a small conical pit at the base of the original pit. The shallow pits associated with short ridges (C in Fig. 5) retain their shape but a new conical pit forms at the opposite end of the ridge (C in Fig. 5b). This conclusively establishes a 1 : 1 relationship between the two etchants as the etch feature produced in solution A–B correlates with the feature produced in solution H. In fact all the short ridge features develop conical pits at one end (D in Fig. 5b).

3.4. Correlation with X-ray topography

The use of X-ray transmission topography and subsequent combination etching of the topographed sample allows a direct correlation of the etch features and dislocation structures to be

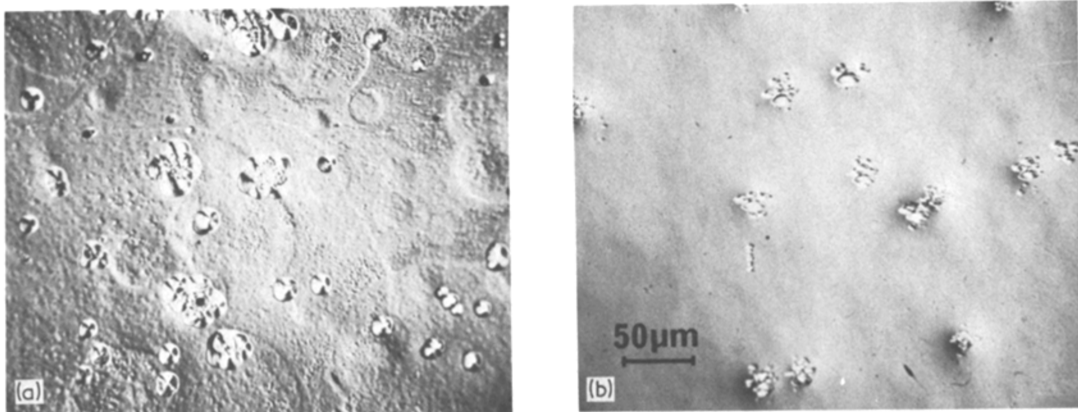

Figure 11 Cluster of etch pits revealed by etching in (a) solution H for 1.5 min on a {100} slice taken from an undoped ⟨100⟩ axis crystal, (b) solution A–B for 60 min on a longitudinal {110} surface from the same undoped ⟨100⟩ axis crystal.

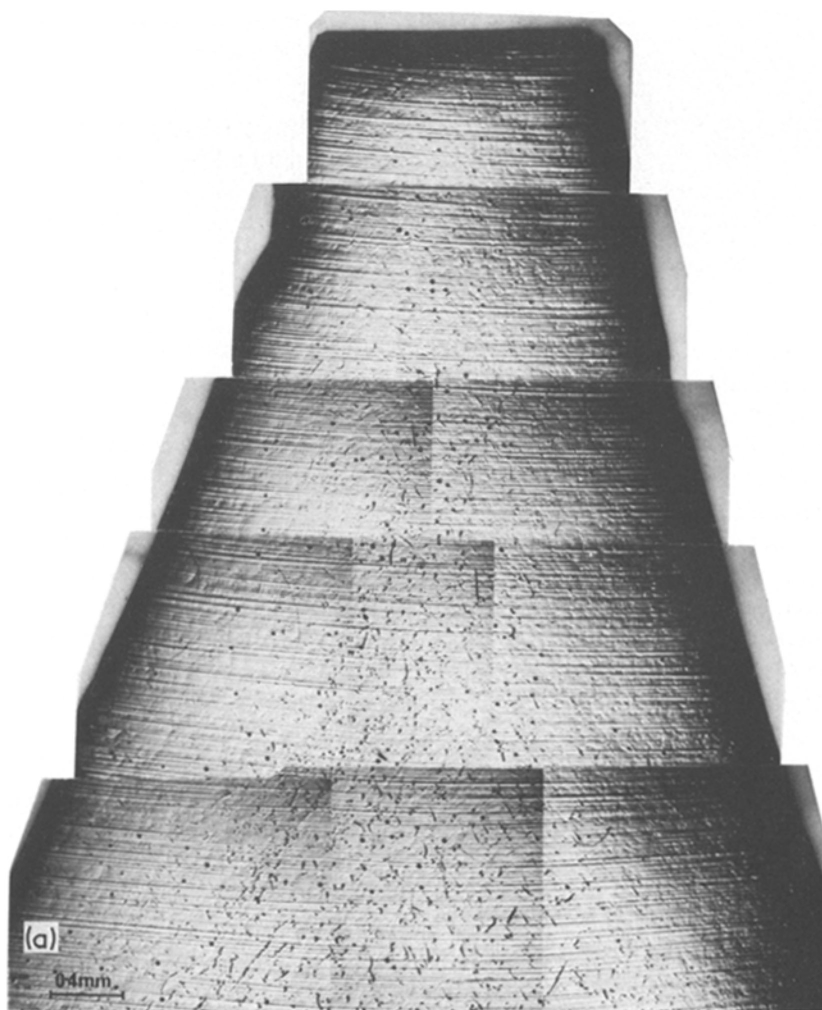

Figure 12 Growth striations delineating the growth interface produced on a longitudinal {1 1 0} surface by etching in solution A–B for 60 min at 60° C for (a) a Ge-doped ⟨1 1 1⟩ axis crystal; small diameter (1.5 cm), (b) a Sn-doped ⟨1 1 1⟩ axis crystal; large diameter (3 cm).

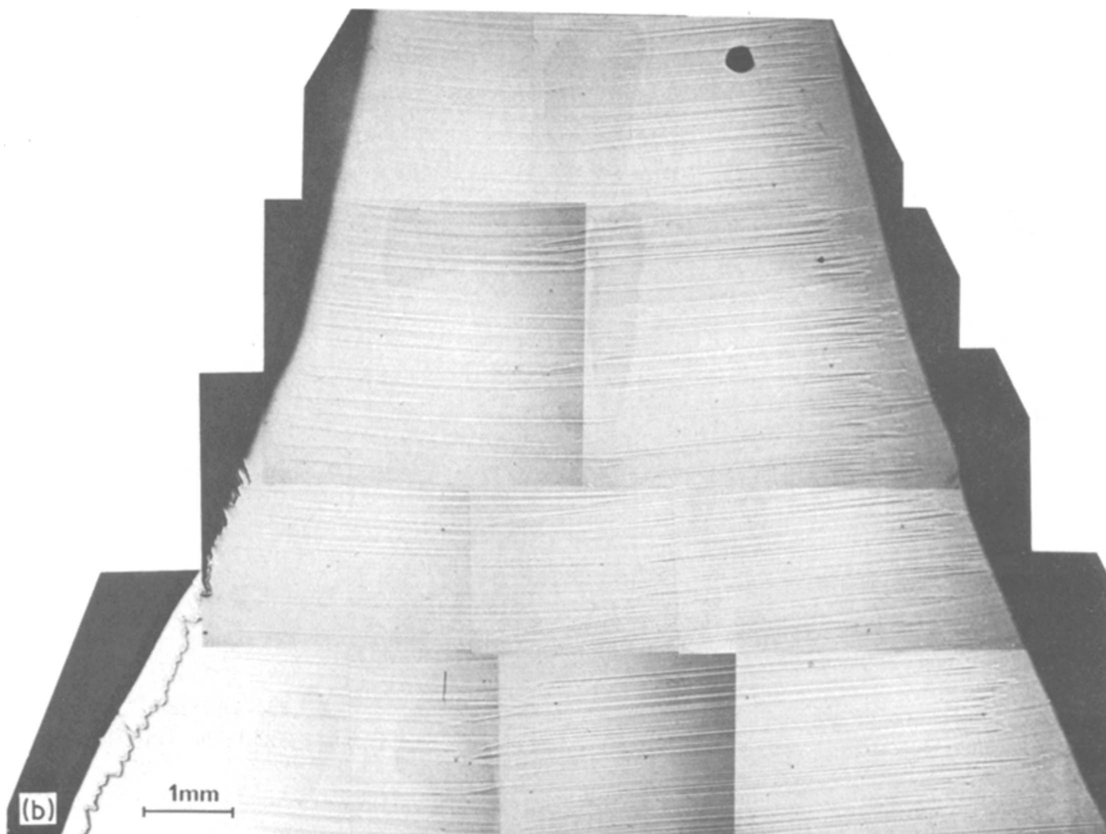

Figure 12 Continued.

made. A topograph for a ⟨1 0 0⟩ slice taken from a ⟨1 1 1⟩ axis Ge-doped crystal is shown in Fig. 10a. After etching in solution H, some of the pits can be correlated with the ends of dislocation lines on the topograph; some of these are marked in Fig. 10b. It can be seen that pits 1 and 2 correspond to both ends of the same dislocation line whilst pit 4 is the point of emergence of a dislocation which lies almost parallel to the surface (the line stretching from top to bottom to the left of pits 3, 4 and 5 is a scratch). Pit 6, on the other hand, correlates with a dot of contrast on the topograph and is likely to be a dislocation orientated perpendicular to the surface. Further etching of this slice in A–B solution again shows a correlation of these pits with etch-memory ridge features and establishes that the ridge features delineate an associated dislocation line. For example, the ridge features emanating from pits 1 and 2 (Fig. 10c) correspond to the dislocation line between these pits (Fig. 10a). Ridge features also extend along the dislocation lines associated with pits 3, 4 and 5 (Figs. 10a and c). No ridge is associated with pit 6 which confirms its association with a dislocation whose line direction is perpendicular to the surface.

4. General etch features

In addition to delineating the general distribution of pits shown in Figs. 1a and b and the amplification of these structures described, the etchants described above show that marked differences can exist between crystals. For example, clusters of pits can sometimes be observed in both horizontal and vertical crystal sections (Figs. 11a and b). Such a distribution is characteristic of dislocations generated at an inclusion, but as yet no positive identification of an inclusion has been obtained in this instance.

The striations present show that marked changes in interface shape can occur. In small diameter crystals, the interface tends to be convex toward the melt (Fig. 12a) but in larger diameters, a large facet can develop (Fig. 12b). The striations are most marked in doped crystals which is to be expected since impurity incorporation is growth rate dependent and striations represent fluctuations in impurity concentration. However, the

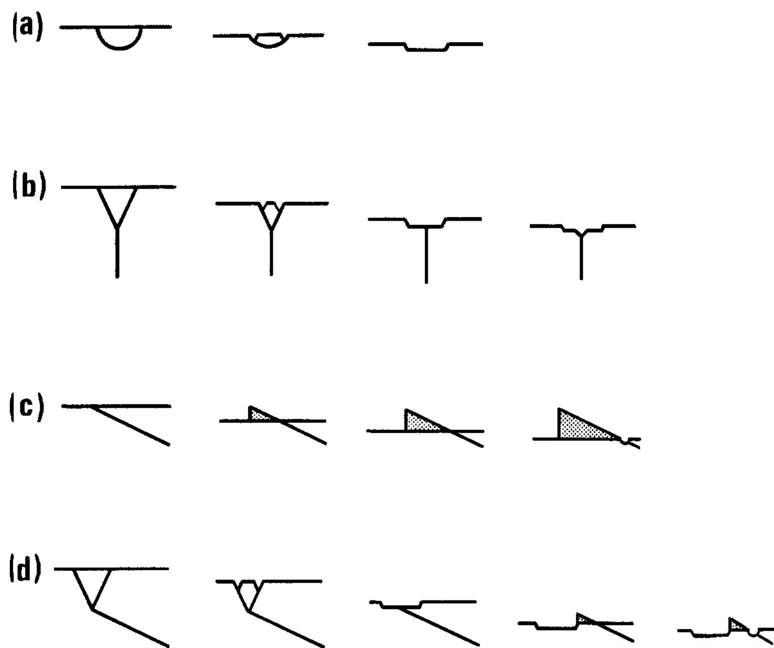

Figure 13 Schematic representation of etching behaviour for particular dislocation configurations (a) a dislocation loop produces a flat bottomed pit, (b) a dislocation node produces a flat bottomed pit and a steeply inclined dislocation meeting the node produces a conical pit on the bed of a flat bottomed pit, (c) a dislocation inclined to the surface produces a ridge feature in solution A–B. Subsequent etching in solution H produces a pit where the dislocation emerges at the surface, (d) a dislocation node with a dislocation inclined to the surface produces a flat bottomed pit with an associated ridge in solution A–B. Subsequent etching in solution H produces a pit where the dislocation emerges at the surface.

presence of striations in undoped material which has been pulled twice in order to improve stoichiometry suggests that very small quantities of impurity or deviation from stoichiometry still exist in the material. These results are a very limited analysis of crystal defect distribution but serve to illustrate that large differences in defect distribution can be found between ostensibly similar crystals; such behaviour could have a marked effect upon the performance of crystal slices used as substrates in device technology.

5. Discussion

The features revealed by etching in either A–B or H solutions may be summarized as follows.

(i) Conical and flat bottomed pits, observed on {1 1 1}P and {1 0 0} surfaces with solution H and on {1 1 1}P surface with A–B solution.

(ii) Etch-memory ridge features, which are the predominant feature produced on {1 0 0} but which also appear to a lesser degree on {1 1 1}P when these surfaces are etched in A–B solution.

(iii) Ridge features associated with flat bottomed pits which are observed on {1 1 1}P surfaces after etching in A–B solution.

(iv) Growth striations, which are revealed by A–B solution.

(v) Faceted hillocks, which are revealed by solution H when mixed using low purity orthophosphoric acid.

Features (i) to (iii) show a marked similarity to the features produced in GaAs with A–B solution. For GaAs the conical pits have been associated with dislocations with a line direction normal, or almost normal to the surface [7]. Similarly, flat bottomed pits have been ascribed to etching through a dislocation loop whose plane is inclined to the surface [12–14] (Fig. 13a). This implies that it should be possible to etch completely through the loop resulting in the complete removal of the pit. In the present experiments it was found that flat bottomed pits persisted even after 20 μm of material has been removed by solution H (the etch-memory effect exhibited by solution A–B suggests that etching through defects is less likely from this etchant). This is unexplained but must mean that if loops are responsible for flat bottomed pits they must either have an extensive strain field or that the etch time required to restore the surface to its equilibrium shape is quite high. However from Fig. 3 it is clear that successive etching of {1 1 1}P surface in A–B solution produces an increase in the density of flat bottomed pits which means that these pits must be associated with loops or precipitates. Some flat bottomed pits develop conical pits on the bed of the pit which increase in size with continued etching (B in Fig. 5) and eventually engulf the original pit. This suggests that the original flat bottomed pit was created by etching through a dislocation node (Fig. 13b).

The development of etch-memory features

with A–B solution is also analogous to GaAs where the features have been correlated with dislocations using X-ray topography [10]. The occurrence of etch ridges is obviously due to a slower etch rate at the defect than on the defect-free surface. However, the {1 1 1}P surface shows both etch-memory ridges and pits (Fig. 5). This may be explained in terms of the orientation of the dislocations with respect to the surface. Where a dislocation line is perpendicular to the surface, the etch rate at the dislocation is greater than that of the surface and a pit is formed. However where a dislocation line is almost parallel to the surface, the surface etches at a greater rate than the dislocation and a ridge is formed. This situation can be described as

$$E_{\theta=90}^{\text{disloc}} > E_{\{111\}\text{P}}^{\text{surface}} > E_{\theta=0}^{\text{disloc}}$$

where E is the etching rate and θ is the angle between the dislocation line and the surface. For the {1 0 0} surface where ridge features are prevalent

$$E_{\{100\}}^{\text{surface}} > E_{\theta=0\rightarrow 90}^{\text{disloc}}.$$

Measurements of etching rates made by masking part of the surface and measuring the heights of steps produced by etching with a Talysurf, gave values for $E_{\{111\}\text{P}}^{\text{surface}}$ and $E_{\{100\}}^{\text{surface}}$ of 0.12 and 0.24 μm min^{-1}, respectively, for etching at 60° C. On this basis, the ridge feature in Fig. 5c corresponds to a dislocation whose line direction is inclined acutely to the surface (Fig. 13c) and the feature marked C in Fig. 5 where a flat bottomed pit and ridge are combined would correlate with the emergence of a node at the end of an inclined dislocation (Fig. 13d). The formation of conical pits at the end of ridge features when etching in solution H implies a lower sensitivity of etch rate to dislocation line orientation for this solution.

The above argument excludes effects due to dislocation decoration by precipitates which occurs in GaAs [11]. The ridge features produced in InP are generally devoid of pit decoration; Fig. 7 shows the only case where this decoration was observed and then only in material grown from an indium-rich melt. However, thus far, the current work has not included the examination of the high dopant levels for which this effect was prevalent in GaAs.

6. Conclusions

Etching of InP in solutions H and A–B has demonstrated that the etching behaviour of these two etchants is quite different. Solution H shows up conical and flat bottomed pits on both {1 1 1}P and {1 0 0} surfaces whereas A–B solution shows up conical and flat bottomed pits and ridge features on {1 1 1}P and only ridges features on {1 0 0} surfaces. The use of combination etching shows that the conical and flat bottomed pits produced on {1 1 1}P by solution H correlate with those produced by solution A–B. However, the ridge features produced by solution A–B etch as conical pits in solution H are indistinguishable from other conical pits. X-ray topography has demonstrated that these etch features are associated with dislocations. The usefulness of these etchants in assessing defect distributions in single crystals is demonstrated.

Acknowledgements

The authors would like to express their gratitude to D. J. Stirland and M. J. Cardwell of Plessey (Caswell) Ltd. for helpful suggestions and stimulating discussion, and to K. H. Lloyd for his assistance with the X-ray topography. The help of E. J. Bullen and Miss S. J. Ruddock with the specimen preparation is also gratefully acknowledged.

References

1. D. J. STIRLAND and B. W. STRAUGHAN, *Thin Solid Films* **31** (1976) 139.
2. J. B. MULLIN, A. ROYLE and B. W. STRAUGHAN, Proceedings of the International Symposium on GaAs, Aachen, 1970 (Inst. of Physics and Phys. Soc., London) p. 41.
3. R. C. CLARKE, D. S. ROBERTSON and A. W. VERE, *J. Mater. Sci.* 8 (1973) 1349.
4. A. HUBER and N. T. LINH, *J. Crystal Growth,* **29** (1975) 80.
5. K. AKITA, T. KUSUNAKI, S. KOMIYA and T. KOTAN, *ibid.* **46** (1976) 783.
6. M. S. ABRAHAMS and C. J. BUIOCCHI, *J. Appl. Phys.* 36 (1965) 2855.
7. W. BARDSLEY, G. W. GREEN, C. H. HOLLIDAY, D. T. J. HURLE, G. C. JOYCE, W. R. MACEWAN and P. J. TUFTON, *Inst. Phys. Conf. Series* **24** (1975) 355.
8. G. T. BROWN, B. COCKAYNE and W. R. MACEWAN, *J. Mater. Sci.* **15** (1980) 1469.
9. P. PENNING, *Philips Res. Repts.,* **13** (1958) 79.
10. D. J. STIRLAND and R. OGDEN, *Phys. Status Solidi (a)* 17 (1973) K1.
11. D. J. STIRLAND, P. D. AUGUSTUS and B. W. STRAUGHAN, *J. Mater. Sci.* **13** (1978) 657.
12. D. J. STIRLAND, private communication.
13. W. G. JOHNSTON and J. J. GILMAN, *J. Appl. Phys.* 30 (1959) 129.
14. C. WERKHOVEN, C. VON OPDORP and A. T. VINK, *Philips Tech. Rev.* **38** (1978/9).

Received 8 February and accepted 4 March 1980.